Journal of Biological Dynamics

ISSN: 1751-3758 (Print) 1751-3766 (Online) Journal homepage: http://www.tandfonline.com/loi/tjbd20

Determining drug efficacy parameters for mathematical models of influenza

Noah F. Beggs & Hana M. Dobrovolny

To cite this article: Noah F. Beggs & Hana M. Dobrovolny (2015) Determining drug efficacy parameters for mathematical models of influenza, Journal of Biological Dynamics, 9:sup1, 332-346, DOI: 10.1080/17513758.2015.1052764

To link to this article: http://dx.doi.org/10.1080/17513758.2015.1052764

Journal of Biological Dynamics, 2015
Vol. 9, Suppl. 1, 332–346, http://dx.doi.org/10.1080/17513758.2015.1052764

Determining drug efficacy parameters for mathematical models of influenza

Noah F. Beggs[a,b] and Hana M. Dobrovolny[b*]

[a]*Department of Biology, Hendrix College, Conway, AR, USA;* [b]*Department of Physics & Astronomy, Texas Christian University, Fort Worth, TX, USA*

(*Received 2 March 2014; accepted 13 May 2015*)

Antivirals are the first line of defence against influenza, so drug efficacy should be re-evaluated for each new strain. However, due to the time and expense involved in assessing the efficacy of drug treatments both *in vitro* and *in vivo*, treatment regimens are largely not re-evaluated even when strains are found to be resistant to antivirals. Mathematical models of the infection process can help in this assessment, but for accurate model predictions, we need to measure model parameters characterizing the efficacy of antivirals. We use computer simulations to explore whether *in vitro* experiments can be used to extract drug efficacy parameters for use in viral kinetics models. We find that the efficacy of neuraminidase inhibitors can be determined by measuring viral load during a single cycle assay, while the efficacy of adamantanes can be determined by measuring infected cells during the preparation stage for the single cycle assay.

Keywords: adamantanes; neuraminidase inhibitors; influenza; mathematical model; antiviral efficacy

AMS Subject Classification: 92C08; 92C50

1. Introduction

Influenza is an infectious disease that can cause serious illness and death. Influenza mutates rapidly [16] and has the ability to recombine to form new strains [29]. The genetic drift caused by single amino acid mutations can lead to mismatch between the vaccine strains and circulating strains of seasonal influenza [4,11,17]. Particularly concerning are the mutations that confer drug resistance [1,7,10,20,26,28], as they will require a change in treatment strategy. In addition to genetic drift, influenza can experience large genetic changes through reassortment [50,61], such as those that led to the 2009 H1N1 pandemic [56]. Given the mismatch between vaccine and circulating strains and the several month-long production time of vaccines, drugs are usually the first line of defense against influenza.

There are two main types of drugs used to fight influenza infections: neuraminidase inhibitors (NAIs) and adamantanes. NAIs prevent neuraminidase from cleaving the virions from the cell, reducing the rate at which virus is released from an infected cell [2,20]. NAIs also increase

*Corresponding author. Email: h.dobrovolny@tcu.edu
Author Email: noah.beggs@ymail.com

virion mobility by preventing the virions from sticking to each other and surrounding mucus [14,45]. Adamantanes reduce the infection rate by blocking uncoating of the influenza virus once it enters the cell, preventing it from ejecting its genetic code into the cell to be transcribed into new virions [1]. Prophylactic treatment with both classes of drugs has been shown in studies to be effective in preventing influenza infections, with NAIs ranging from 58% to 84% efficacy [40] and adamantanes having a 61% efficacy [39].

Efficacy of the drugs, however, is known to be dependent on viral strain [19,47]. *In vitro* assays are often used to assess the efficacy of antivirals against circulating strains [37]. Measurements of how viral load [52] or cytopathic effect [47] change with increasing dose of antiviral are used to help determine whether a particular strain is drug resistant. Unfortunately, researchers are not consistent in the type of *in vitro* assay used or even in the experimental measurement that is used to characterize drug efficacy. This makes it difficult to interpret and compare results from different studies and to extrapolate what these results would mean for patient treatment options.

Mathematical modelling can play an important role in this process by allowing investigators to judge the effect of novel regimens, such as combination therapy, before clinical implementation. Mathematical models of influenza viral kinetics have already been used in this way to show that delayed treatment with oseltamivir could be effective in treating long-lasting influenza [15], but is likely to have limited efficacy for seasonal influenza [12,15]. Another modelling study examined the effect of several hypothetical antivirals, each targeting a different part of the replication cycle, to determine which would be most effective at reducing viral titers [31]. While the use of mathematical models to design influenza drug treatment is still quite new, drug regimen optimization using mathematical models is more common for other infectious diseases [9,48] including HIV [3,23,42,63], hepatitis B [54], and hepatitis C [22].

In order for mathematical models to accurately predict treatment outcomes, drug efficacy parameters must be properly measured. The two key measures of the efficacy of a drug are the 50% inhibitory concentration (IC_{50}) and the maximum antiviral efficacy (ε_{max}). The IC_{50} is the concentration at which the antiviral inhibits an infection parameter (e.g. viral production rate or virion infectivity) to 50% of its value in an untreated infection. ε_{max}, a number between 0 and 1, describes the maximum inhibition possible when the antiviral is applied at saturation concentrations. It is important to note, however, that the values of these parameters will depend on the quantity being measured [55]. For example, while it is quite clear that NAIs are highly effective (near 100%) at inhibiting the activity of neuraminidase [41,57,62], this does not necessarily translate to the same high efficacy at preventing infections. When given *in vivo*, several factors diminish the effectiveness of NAIs, including bioavailability [13,30] and alternative viral release pathways [21,36,43]. This affects not just the measured ε_{max}, but also the measured IC_{50}; hence, the distinction usually made between a 50% inhibitory concentration and a 50% effective concentration (EC_{50}) which measures a drug's effect on a more large-scale process [18].

For viral kinetics models, these different values for ε_{max} and IC_{50} pose a problem. Most viral kinetics models do not explicitly model the action of neuraminidase or the uncoating of virions, but rather include these biochemical processes as part of larger processes. Since the biochemical processes are not explicitly included in the model, the effect of a drug is applied to the larger process. For example, NAIs are often modelled as reducing the production rate [5,15,25], a process that includes production, assembly and release of virions, even though NAIs only block release of the virus. Likewise, although adamantanes block viral uncoating, their effect is modelled as reducing the infection rate [8] which also includes processes such as viral attachment and viral entry into the cell. This means that we cannot assume that the IC_{50} and ε_{max} measured in inhibition assays are the correct parameters for use in a viral kinetics model since inhibition assays only measure the biochemical effect of the drug. Similarly, we cannot assume that EC_{50} and ε_{max} measured from *in vitro* or *in vivo* infections will provide the correct values for use in a viral kinetics model since these characterize the effect of the drug on quantities derived from

multiple cycles of infection. In order to effectively use viral kinetics models, however, we need to determine the correct values of IC_{50} and ε_{max} for use in the model.

This paper uses computer simulations to examine whether there are any experimental measurements that can determine the proper IC_{50} and ε_{max} values for modelling NAIs and adamantanes in a viral kinetics model. We find that the IC_{50} and ε_{max} for modelling NAIs can be extracted from a single cycle assay while the IC_{50} and ε_{max} for adamantanes can be extracted from an assay that isolates the infection process.

2. Methods

2.1. *Mathematical model*

We use an extension of the mathematical model presented in Baccam *et al.* [5] to simulate the influenza life cycle,

$$\begin{aligned}
\frac{dT}{dt} &= -\beta TV,\\
\frac{dE_1}{dt} &= (1-m)\beta TV - \frac{n_E}{\tau_E}E_1,\\
\frac{dE_j}{dt} &= \frac{n_E}{\tau_E}E_{j-1} - \frac{n_E}{\tau_E}E_j \quad \text{for } j = (2,\ldots,n_E),\\
\frac{dI_1}{dt} &= \frac{n_E}{\tau_E}E_{n_E} - \frac{n_I}{\tau_I}I_1,\\
\frac{dI_j}{dt} &= \frac{n_I}{\tau_I}I_{j-1} - \frac{n_I}{\tau_I}I_j \quad \text{for } j = (2,\ldots,n_I),\\
\frac{dV}{dt} &= (1-n)p\sum_{j=1}^{n_I} I_j - cV.
\end{aligned} \tag{1}$$

In the model, target cells, T, become infected at rate β when they encounter virus. Upon infection, the cells enter an eclipse state, E, where they are infected, but not yet producing virus. After an average time, τ_E, the cells transition to a productively infectious state, I, where they are producing virus at rate p. After an average time, τ_I, the infectious cells die. Virus loses infectivity at a rate c. A schematic of the model is shown in Figure 1. Parameters were taken from previously published fits to experimental data from the pandemic H1N1 virus [49]. Parameters are listed in Table 1.

Since adamantanes prevent uncoating of the virion, the effect of adamantanes is modelled as reducing the infection rate β with efficacy m in the equation for E only. Beauchemin *et al.* [8] showed that this formulation more accurately reproduced the effect of amantadine than applying the drug effect to β in both the T and E equations. In the above formulation, target cells are removed from the population when an infectious virus enters the cell. This prevents possible multiple infections of a single cell in the presence of amantadine. The effect of NAIs is modelled as reducing the production rate p with efficacy n. In this formulation, we are assuming that NAIs prevent formation of virions rather than just block release of fully formed virions.

Our model assumes a gamma distribution, represented by the multiple compartments for E and I, for the transition times between the eclipse state and the infectious state, as well as for the transition times between the infectious and dead cells. The number of compartments in the eclipse state is given by n_E, while the number of compartments in the infectious state is given

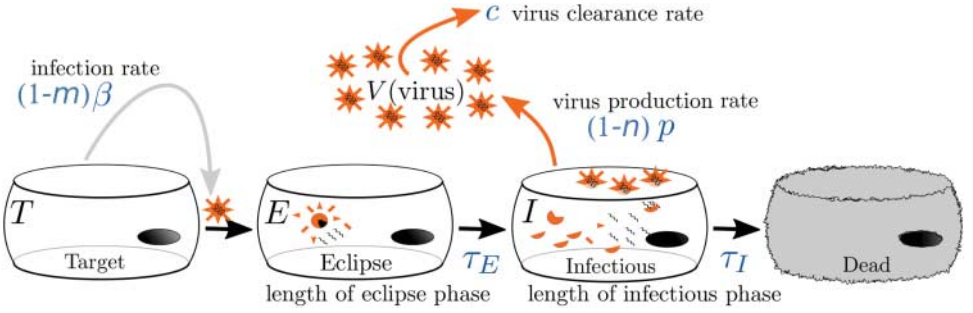

Figure 1. Influenza infection model. The virus, V, attacks target cells, T, at rate β. Once infected, target cells enter the eclipse phase, E. The eclipse phase lasts an average time of τ_E, after which the cells become infectious cells, I. The infectious cells produce new virions at rate p, and the virus decays at rate c. The cells remain infectious for an average time of τ_I, after which they become dead cells. Adamantanes reduce β with efficacy m, and NAIs reduce p with efficacy n.

Table 1. Parameter values for model (1).

Parameter	Value
β	426 $(\text{h} \cdot \text{pfu/mL})^{-1}$
p	176 $\text{pfu/mL} \cdot \text{h}^{-1}$
τ_E	6.6 h
τ_I	49 h
c	0.13 h^{-1}
n_E	30
n_I	100
$\varepsilon^*_{\max}$	0–1
IC^*_{50}	varies

Note: Values are taken from [49].
* When $\varepsilon_{\max}$ and IC_{50} are not varied, they are fixed at 1.

by n_I. The gamma distribution avoids the very short or very long transition times allowed by an exponential model. Previous work has shown that the exponential model does not properly model a single cycle assay [34], which is one of the assays we simulate.

2.2. *Implementing the effect of drugs*

In the model, we use the efficacy of a drug to reduce either the infection rate or the production rate. In experiments, however, researchers apply a particular dose, D, of a drug. We can relate the dose of a drug to its efficacy through the $E_{\max}$ model [35],

$$\varepsilon = \varepsilon_{\max} \frac{D^\gamma}{\text{IC}_{50}^\gamma + D^\gamma}, \tag{2}$$

where $\varepsilon_{\max}$ is the maximum effect of the drug, IC_{50} is the drug concentration at which the drug achieves 50% of its maximum effect, and γ controls the steepness of the sigmoidal function. Biologically, γ is determined by the number of binding reactions needed for the drug to function [60]. Many drugs require only one binding reaction, so a large number of dose–response curves are adequately fit with $\gamma = 1$. We have assumed that this is the case for both NAIs and adamantanes.

2.3. *Simulating experimental assays*

Simulation of experimental assays is implemented in the model by changing the initial conditions to reflect the initial conditions for *in vitro* assays. We initially explore two common *in vitro* assays: the multiple cycle assay and the single cycle assay.

Perhaps the most common *in vitro* assay is the multiple cycle assay, pictured in Figure 2 (top). Experimentally, initial conditions are presented in terms of the multiplicity of infection (MOI). The MOI is the ratio of virus to target cells. In the multiple cycle experiment, virus at a low MOI is allowed to incubate on a cell culture for 1 h. After the incubation period, the seed virus is washed off. Since the MOI is low, only a small fraction of cells is infected during the incubation period. We can assume that the initially infected cells will be in the eclipse phase as the eclipse phase duration lasts, on average, 6 h [5], so the infected cells will not yet have had time to become productively infectious. These cells initiate an infection which is monitored by measuring the amount of virus in the supernatant or the fraction of dead cells at various times. We simulate this type of assay by adjusting the initial conditions for our model. We assume that there are 10^6 cells in the *in vitro* preparation. We start the simulation after the seed virus has been washed off, so we assume that $V_0 = 0$. The number of cells initially in the first eclipse compartment is assumed to be 50, as in Pinilla *et al.* [49]. There are initially no cells in the remaining eclipse compartments or in any infectious compartments.

Another type of *in vitro* assay is the single cycle assay, pictured in Figure 2 (bottom). In this experiment, a high MOI (> 1) is allowed to incubate on a cell culture for 1 h. After the incubation period, the seed virus is washed off. Since the MOI for this experiment is high, we assume that all cells in the well have been infected during the incubation period. We again assume that all infected cells are in the eclipse state since the 1 h incubation period is shorter than the assumed mean 6 h duration of the eclipse phase. We simulate this assay by assuming that all the seed virus has been washed off ($V_0 = 0$) and that all the cells in the well have been infected. We again assume that the infected cells are in the first eclipse compartment and that the remaining eclipse compartments and infectious compartments initially are zero. Since all cells are infected, the initial number of target cells is zero.

2.4. *Assessing drug efficacy*

The goal of our research is to determine whether any experimentally measurable quantities actually correspond to the underlying IC_{50} and ε_{max}. We investigate this possibility through a simulation study exploring the manifestation of drugs on several quantities that can be measured from *in vitro* assays. When studying infection dynamics, researchers most often measure viral

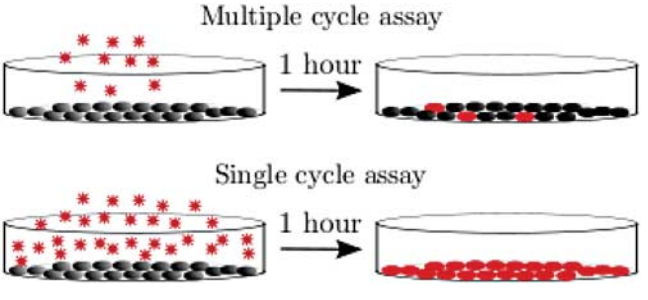

Figure 2. Experimental *in vitro* assays. (top) The multiple cycle assay is initiated with a small amount of virus. After the 1 h incubation period, the initial viral inoculum is washed off, leaving a small number of infected cells. (bottom) The single cycle assay is initiated with a large amount of virus. After the 1 h incubation period, the initial viral inoculum is washed off, leaving all the cells in the well infected.

load as a function of time [52], but the cytopathic effect (number of dead cells) is also a common measurement, particularly when assessing the effect of an antiviral [46]. We predict the effect of the drug on several characteristics of the viral titer and dead cell time courses. We first assess the effect of the drug on viral titer measured at a particular time; perhaps the most common experimental method for assessing the efficacy of a drug. Several different measurement times are investigated. We also study the effect of the drug on peak viral titer, time of viral peak, viral upslope, viral downslope and area under the curve (AUC). AUC is the area under the viral titer curve and is often used to assess the severity of an infection [6,27]. Viral upslope is the exponential growth rate of the viral titer during the first ~ 1 d of infection. The viral downslope is the exponential decay rate of the viral titer. While these quantities are not typically measured experimentally, they can be determined from experimental data and it is worth investigating whether they can be used to extract model parameters. Additionally, we examine the number of dead cells at a specific time; again a common method of assessing the efficacy of a drug. For the dead cells, we also investigate the time at which half the maximum number of dead cells have died. This is again a quantity that is not typically measured, but one that can be extracted from experimental data and might be useful for determining model parameters.

To determine whether any of these predicted outcomes can extract model drug efficacy parameters, we use the following procedure:

(1) We simulate both the multiple cycle and single cycle assays for a variety of $\varepsilon_{\max}$ and IC_{50} values. When $\varepsilon_{\max}$ is varied, IC_{50} is held fixed at 1 and when IC_{50} is varied, $\varepsilon_{\max}$ is held fixed at 1.
(2) We generate dose–response curves for each of the quantities discussed above (i.e viral upslope, AUC, etc.) for all $\varepsilon_{\max}$ and IC_{50} values.
(3) From the dose–response curves, we extract the effective $\varepsilon_{\max}$, which we denote ε_{out}, or the effective IC_{50}, which we denote $IC_{50,\text{out}}$.
(4) We plot the effective ε_{out} or $IC_{50,\text{out}}$ as a function of the assumed $\varepsilon_{\max}$ or IC_{50}.

For example, Figure 3 shows dose–response curves generated by measuring the viral titer in a multiple cycle assay at 48 h. To generate the curves, we assumed an IC_{50} of 1 and $\varepsilon_{\max}$ values of 0.2, 0.4, 0.6, and 0.8. The effective ε_{out} and $IC_{50,\text{out}}$ for these measurements are the maximum

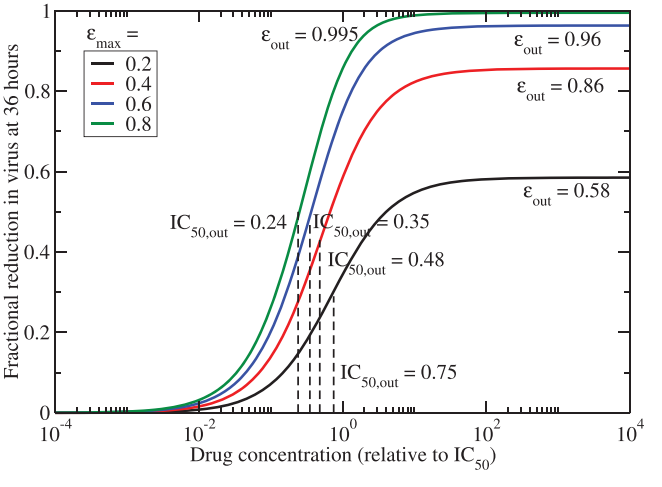

Figure 3. Dose response curves. We simulated a multiple cycle assay and measured the viral load at 48 h as a function of drug concentration. We assumed values of $IC_{50} = 1$ and $\varepsilon_{\max} = 0.2,0.4,0.6,0.8$ to generate the curves, but the dose–response curves produce different effective values of ε_{out} and $IC_{50,\text{out}}$.

effect and 50% effective dose as read off the dose–response curves. Note that in this case, the ε_{out} read off the dose–response curves does not match the ε_{max} value we used to simulate the experiment. Similarly, the $IC_{50,out}$ measured from the different curves changes even though the underlying IC_{50} used for simulations is the same for all curves. If the experimentally measurable quantity reflects the underlying ε_{max} values, then a plot of ε_{max} (input value) versus ε_{out} (output value) or IC_{50} (input value) versus $IC_{50,out}$ (output value) will yield a straight line with a slope of 1.

3. Results

3.1. *Neuramindase inhibitors*

We simulate the multiple cycle assay and determine ε_{out} for several values of ε_{max} and $IC_{50,out}$ for several values of IC_{50} for the experimental measures described in Section 2.4. When varying ε_{max}, we keep IC_{50} fixed to 1, and when varying IC_{50}, we keep ε_{max} fixed to 1. Figure 4 shows ε_{out} (top row) and $IC_{50,out}$ (bottom row) as functions of ε_{max} and IC_{50}, respectively. We see that none of the extracted drug parameters return the original values of ε_{max} or IC_{50}. In fact, most of the input/output relationships are nonlinear. The two exceptions are the peak viral titer and AUC (red and cyan lines in the rightmost graphs) which show a linear relationship, but it does not have a slope of one. This could potentially be used to determine the underlying ε_{max} and IC_{50} if we can ascertain the value of the slope and determine whether it is independent of the type of drug or other factors. It is, however, preferable to find experimentally measurable quantities that can extract the original quantities directly, without having to worry about measuring additional parameters.

It is interesting to note that the values of ε_{out} and $IC_{50,out}$ predicted by viral titer at a particular time or by dead cells at a particular time depend on the chosen measurement time. Since experimentalists often use single time point measurements to assess the efficacy of a drug and to extract EC_{50}, the values of EC_{50} extracted in this way will not be consistent if the time chosen for measurement differs from experiment to experiment. This is particularly problematic since

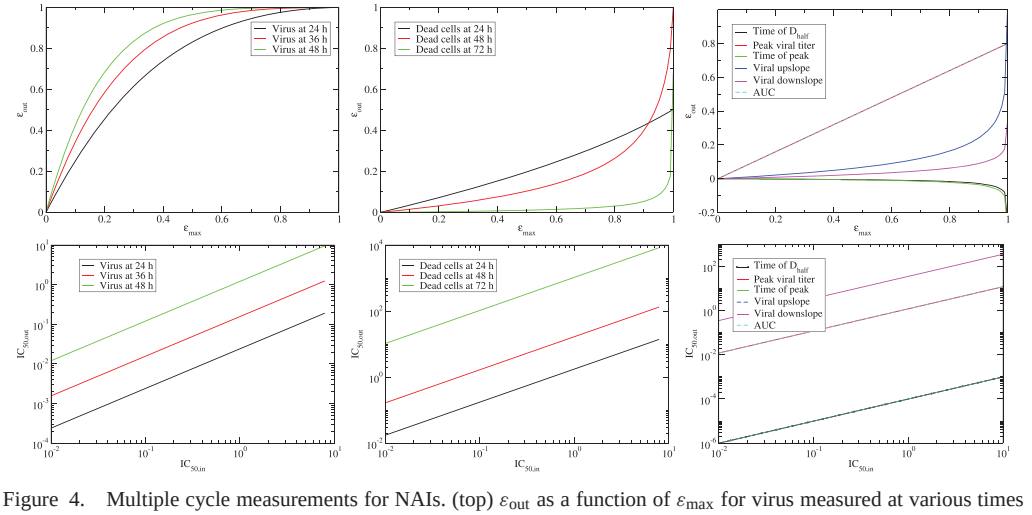

Figure 4. Multiple cycle measurements for NAIs. (top) ε_{out} as a function of ε_{max} for virus measured at various times (left), number of dead cells at various times (centre), and other measurable quantities (right). (bottom) $IC_{50,out}$ as a function of the assumed value of IC_{50} for virus measured at various times (left), number of dead cells at various times (centre), and other measurable quantities (right). None of the measurements produce a line of slope equal to 1 relating the assumed and predicted values.

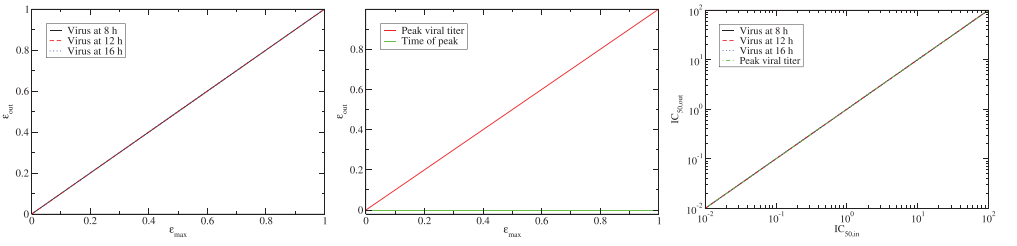

Figure 5. Single cycle measurements for NAIs. We show ε_{out} as a function of ε_{max} for virus measured at various times (left) and other measurable quantities (centre). The rightmost graph shows these same quantities for IC_{50}. Several of the measurements correctly extract the assumed value of ε_{max} as seen by the lines of slope equal to 1.

EC_{50} is the quantity that is typically used to determine whether a particular viral strain is drug resistant [2,10].

Since our simulations of the multiple cycle assay did not yield any quantities that could determine the correct value of ε_{max}, we examined the single cycle assay. Figure 5 shows the predicted values of ε_{out} (left, centre) and $IC_{50,out}$ (right). We do not show the dead cell measurements here because the time course of dead cells is unaffected by the application of NAIs in the single cycle assay. Since all of the cells are infected at the same time and NAIs only alter the production rate of virus, the time course of the cells' infected lifespans will not change with application of the drug. This simulation does result in predictions of measurements that can be used to determine ε_{max} and IC_{50}. In the single cycle assay, the virus measured at any time as well as the peak viral titer will both return the drug efficacy parameters needed for simulation of NAI treatment.

It might seem surprising that we can extract the correct ε_{max} and IC_{50} by measuring virus at any time. To investigate why the result is time-independent, we derived an expression for the virus as a function of time for the single cycle assay (Appendix 1). We find that the virus is linearly proportional to the production rate (Equation (A6)), and consequently it is also proportional to the drug effect. The only assumption used in deriving this result is that the viral loss of infectivity is negligible, so as long as viral titer measurements are made before the viral titer peak, we can extract the IC_{50} and ε_{max} needed for the mathematical model.

3.2. *Adamantanes*

While the single cycle assay provides a method for determining the drug efficacy parameters of NAIs, it does not work for adamantanes. This is because adamantanes affect the infection rate of the influenza virus, but in a single cycle experiment, all cells are already infected when the drug is added. This can also be shown analytically (Appendix 1) since the expression for virus in a single cycle assay (Equation (A6)) is independent of the infection rate β, and so is independent of the effect of adamantanes.

Adamantanes do, however, have an effect on the multiple cycle assay. Figure 6 shows ε_{out} as a function of ε_{max} (top row) and $IC_{50,out}$ as a function of IC_{50} for experimentally measurable quantities of the multiple cycle assay. The multiple cycle assay again does not provide any measurements that can be used to extract ε_{max} or IC_{50}.

Since none of the measurements from the multiple cycle assay can be used to determine the drug efficacy parameters for adamantanes and the single cycle assay also cannot be used, new assays or measurements need to be developed. The single cycle assay can be used to determine the effect of NAIs because it removes the infection process from the experiment, resulting in direct measurements of the production portion of the viral life cycle. For adamantanes, we need an assay that removes the production process, so that we can focus on the infection portion of the viral life cycle. Since the single cycle assay isolates the production process, it stands to reason

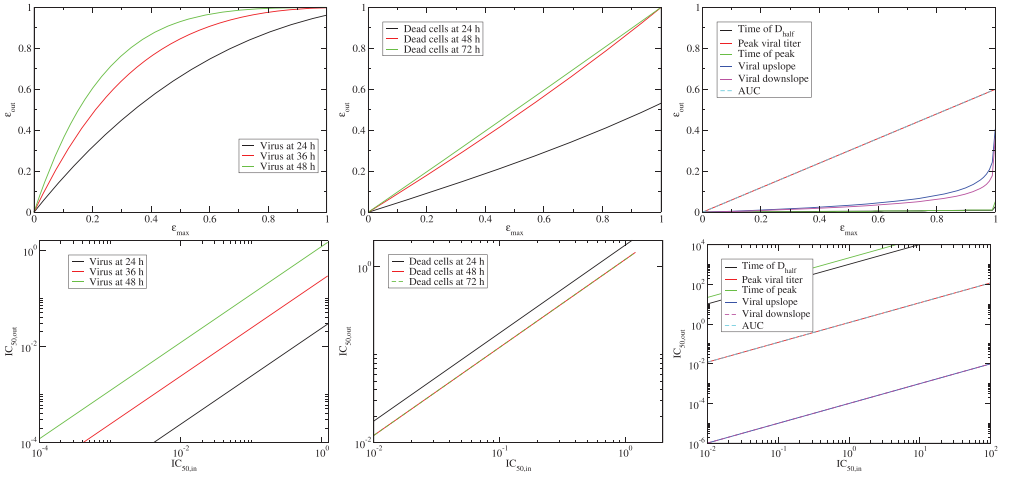

Figure 6. Multiple cycle measurements for adamantanes. (top) ε_{out} as a function of ε_{max} for virus measured at various times (left), number of dead cells at various times (centre), and other measurable quantities (right). (bottom) $IC_{50,out}$ as a function of the assumed value of IC_{50} for virus measured at various times (left), number of dead cells at various times (centre), and other measurable quantities (right). None of the measurements produce a line of slope equal to 1 relating the assumed and predicted values.

that the incubation period for the single cycle assay isolates the infection process, so we propose the following 'incubation assay'. Experimental implementation of the incubation assay involves study of the incubation period of the single cycle assay. Remember that in the incubation part

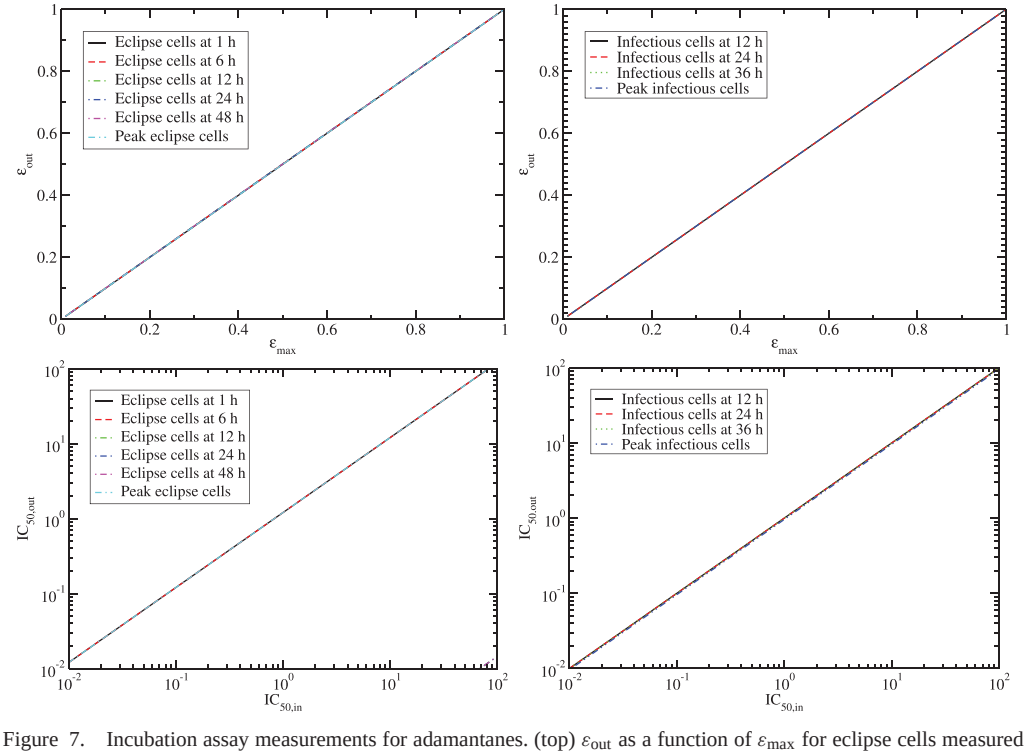

Figure 7. Incubation assay measurements for adamantanes. (top) ε_{out} as a function of ε_{max} for eclipse cells measured at various times (left) and infectious cells measured at various times (right). (bottom) $IC_{50,out}$ as a function of IC_{50} for eclipse cells measured at various times (left) and infectious cells measured at various times (right). All the measurements result in the correct extraction of the assumed values of ε_{max} and IC_{50}.

of the experiment, virus at a high MOI is allowed to infect cells in the well. In the proposed incubation assay, virus at a high MOI is placed in a well of susceptible cells. Unlike the single cycle and multiple cycle assays, however, the initial viral inoculum is not removed after 1 h, but is allowed to remain in the well for the duration of the experiment. Rather than measure virus or the number of dead cells, it makes sense to study the number of infected cells since we do not want to include any of the production process in our measurements.

We simulate the incubation period by assuming the initial amount of virus is high (MOI of 4) [49] and that no cells are initially infected ($T_0 = N$, $E_0 = 0$, $I_0 = 0$). We study the cells in the eclipse state or cells in the infectious state at several time points. We also examine the peak number of eclipse cells and the peak number of infectious cells. While experimentalists do not often measure infected cells, such measurements are feasible with today's technology [44,51,59].

Figure 7 shows the ε_{out} (top row) and $IC_{50,out}$ (bottom row) determined from measurements of the number of eclipse cells (left) or the number of infectious cells (right). As we saw for the virus in single cycle assays and NAIs, determining the correct ε_{max} and IC_{50} using eclipse or infectious cells is independent of the measurement time, making it easy for experimentalists to make this measurement. The key to determining drug efficacy parameters is to find an experimentally measurable quantity that is linearly proportional to the drug efficacy. For the incubation assay proposed here, we can show that both the eclipse cells and the infectious cells are linearly proportional to the applied drug effect for adamantanes (Appendix 2).

4. Discussion

Our work predicts that *in vitro* assays can be used to extract the values of ε_{max} and IC_{50} needed to simulate influenza treatment with either NAIs or adamantanes. In addition to simulation results, we derived analytical results showing that ε_{max} and IC_{50} can be determined from experimental *in vitro* assays. Unlike the work of Heldt *et al.* [31], who examined the effect of drugs that have not yet been developed, our study characterizes the effect of antivirals that are currently in use. Our results show how to correctly parameterize antiviral drug effects for a particular strain of influenza, so that the effect of NAIs and adamantanes can be accurately modelled.

We find that the most common experimental assay, the multiple cycle assay, cannot be used to extract parameters for either NAIs or adamantanes. It is likely that the multiple cycle assay fails to provide a direct reflection of the drug effect of either adamantanes or NAIs since both infection and production processes are part of the multiple cycle assay making it difficult to isolate the effect of a drug acting at only one of those parts of the replication cycle.

The experiment that allows us to determine the ε_{max} and IC_{50} for NAIs is the single cycle assay, an *in vitro* assay that is already widely used to assess viral replication [24,49,58]. Measuring peak virus will return the correct ε_{max} and IC_{50}, but this is a property that is difficult to measure accurately with current *in vitro* assays. Fortunately, virus measured at any time, at least before viral clearance becomes significant, will also return the correct ε_{max} and IC_{50}. This measurement does not involve any new techniques or experimental methods [32,33] and so should be easy for experimentalists to measure. The data can be collected as part of standard experiments that determine the efficacy of NAIs against new strains of influenza. This is particularly important for NAIs since oseltamivir, an NAI, is the drug most often stockpiled in preparation for a pandemic [53]. Rapid determination of drug efficacy parameters during a pandemic will allow us to identify drug-resistant strains. We can then use the parameters in a viral kinetics model to help assess whether the NAI will be an effective treatment, helping to guide public health authorities in their decisions on how to distribute drugs within the stockpile.

Determining ε_{max} and IC_{50} for adamantanes is more complex, but still feasible with modern methods. Our proposed new assay is part of the preparation for a single cycle assay; we simply

propose measuring during the incubation period. While the required preparation is already commonly used, the measurement needed from this assay is not as common. Most investigations of influenza infections measure virus or sometimes the number of dead cells [55]; it is not very common to measure the number of cells in the eclipse or infectious state. In fact, there are currently no experimental techniques that differentiate between cells in the eclipse phase and cells in the infectious phase, but there are methods that can detect infected cells [44,51,59]. One method uses green fluorescent protein labelling to track viral RNA [44]. The fluorescent label allows researchers to track a virus particle as it travels from the intracellular medium to the cell. Another method uses monoclonal antibodies and immunostaining to co-locate viral proteins and cells [51,59]. Either method could be used to measure the number of infected cells at particular times during the incubation period. While adamantanes are not often used as a primary line of defence, they could play an important role in pandemic planning as part of combination therapy aimed at preventing both spread of the disease and emergence of drug resistance [38]. Mathematical modelling of combination therapy will be particularly helpful for quickly identifying doses of the two drugs that will be most beneficial to patients, making treatment of patients safer and more effective.

It is important to note that the drug efficacy parameters extracted from our proposed *in vitro* assays are limited to use within viral kinetics models. More detailed models that include some of the biochemical processes [31] will implement the effect of antivirals differently and will likely require assays that isolate specific biochemical processes to extract the correct drug efficacy parameters. Nonetheless, since viral kinetics models are still often used to investigate drug treatment strategies, our results will allow modellers to extract the parameters needed for these models. Our investigation of how to extract efficacy parameters for viral kinetics models should, however, provide a guide to approaching the problem of parameter estimation in more detailed models.

Disclosure statement

No potential conflict of interest was reported by the authors.

References

[1] Y. Abed, N. Goyette, and G. Boivin, *Generation and characterization of recombinant influenza A (H1N1) viruses harboring amantadine resistance mutations*, Antimicrob. Agents Chemother. 49 (2005), pp. 556–559.
[2] Y. Abed, A.M. Bourgault, R.J. Fenton, P.J. Morley, D. Gower, I.J. Owens, M. Tisdale, and G. Boivin, *Characterization of 2 influenza A(H3N2) clinical isolates with reduced susceptibility to neuraminidase inhibitors due to mutations in the hemagglutinin gene*, J. Infect. Dis. 186 (2002), pp. 1074–1080.
[3] B. Adams, H. Banks, H. Kwon, and H. Tran, *Dynamic multidrug therapies for hiv: Optimal and sti control approaches*, Math. Biosci. Eng. 1 (2004), pp. 223–241.
[4] N. Andrews, J. McMenamin, H. Durnall, J. Ellis, A. Lackenby, C. Robertson, B. Wissmannvon, S. Cottrell, B. Smyth, C. Moore, R. Gunson, M. Zambon, D. Fleming, and R. Pebody, *Effectiveness of trivalent seasonal influenza vaccine in preventing laboratory-confirmed influenza in primary care in the United Kingdom: 2012/13 end of season results*, Euro. Surveill. 19 (2014), 20851.
[5] P. Baccam, C. Beauchemin, C.A. Macken, F.G. Hayden, and A.S. Perelson, *Kinetics of influenza A virus infection in humans*, J. Virol. 80 (2006), pp. 7590–7599.
[6] L. Barroso, J. Treanor, L. Gubareva, and F.G. Hayden, *Efficacy and tolerability of the oral neuraminidase inhibitor peramivir in experimental human influenza: Randomized, controlled trials for prophylaxis and treatment*, Antivir. Ther. 10 (2005), pp. 901–910.
[7] M. Baz, Y. Abed, J. McDonald, and G. Boivin, *Characterization of multidrug-resistant influenza A/H3N2 viruses shed during 1 year by an immunocompromised child*, Clin. Infect. Dis. 43 (2006), pp. 1555–1561.
[8] C.A. Beauchemin, J.J. McSharry, G.L. Drusano, J.T. Nguyen, G.T. Went, R.M. Ribeiro, and A.S. Perelson, *Modeling amantadine treatment of influenza A virus in vitro*, J. Theor. Biol. 254 (2008), pp. 439–451.
[9] S. Bonhoeffer, R. May, G. Shaw, and M. Nowak, *Virus dynamics and drug therapy*, Proc. Natl. Acad. Sci. USA 94 (1997), pp. 6971–6976.

[10] R.A. Bright, D.K. Shay, B. Shu, N.J. Cox, and A.I. Klimov, *Adamantane resistance among influenza A viruses isolated early during the 2005-2006 influenza season in the United States*, JAMA 295 (2006), pp. 891–894.

[11] J. Cai, X. Wang, B. Zhao, W. Yao, X. Wang, Q. Zhu, and M. Zeng, *Prevalence, genetic drift of haemagglutinin, and antiviral resistance of influenza A/H3N2 viruses circulating in shanghai in children during 2009–2012*, J. Med. Virol. 86 (2014), pp. 628–633.

[12] L. Canini, J.M. Conway, A.S. Perelson, and F. Carrat, *Impact of different oseltamivir regimens on treating influenza A virus infection and resistance emergence: Insights from a modelling study*, PLoS Comput. Biol. 10 (2014), p. e1003568.

[13] L. Cass, C. Efthymiopoulos, and A. Bye, *Pharmacokinetics of zanamivir after intravenous, oral, inhaled or intranasal administration to healthy volunteers*, Clin. Pharmacokinet. 36 (1999), pp. 1–11.

[14] M. Cohen, X.Q. Zhang, H.P. Senaati, H.W. Chen, N.M. Varki, R.T. Schooley, and P. Gagneux, *Influenza A penetrates host mucus by cleaving sialic acids with neuraminidase*, J. Virol. 10 (2013), pp. 321–334.

[15] H.M. Dobrovolny, R. Gieschke, B.E. Davies, N.L. Jumbe, and C.A.A. Beauchemin, *Neuraminidase inhibitors for treatment of human and avian strain influenza: A comparative study*, J. Theor. Biol. 269 (2011), pp. 234–244.

[16] J.W. Drake, *Rates of spontaneous mutation among RNA viruses*, Proc. Natl. Acad. Sci. USA 90 (1993), pp. 4171–4175.

[17] A. Fantoni, C. Arena, L. Corrias, N. Salez, X.N. Lamballeriede, J.P. Amoros, T. Blanchon, L. Varesi, and A. Falchi, *Genetic drift of influenza A(H3N2) viruses during two consecutive seasons in 2011–2013 in Corsica, France*, J. Med. Virol. 86 (2014), pp. 585–591.

[18] E.A. Govorkova, I.A. Leneva, O.G. Goloubeva, K. Bush, and R.G. Webster, *Comparison of efficacies of RWJ-270201, zanamivir, and oseltamivir against H5N1, H9N2, and other avian influenza viruses*, Antimicrob. Agents Chemother. 45 (2001), pp. 2723–2732.

[19] E.A. Govorkova, N.A. Ilyushina, D.A. Boltz, A. Douglas, N. Yilmaz, and R.G. Webster, *Efficacy of oseltamivir therapy in ferrets inoculated with different clades of H5N1 influenza virus*, Antimicrob. Agents Chemother. 51 (2007), pp. 1414–1424.

[20] L.V. Gubareva, L. Kaiser, and F.G. Hayden, *Influenza virus neuraminidase inhibitors*, Lancet 355 (2000), pp. 827–835.

[21] L.V. Gubareva, M.S. Nedyalkova, D.V. Novikov, K.G. Murti, E. Hoffmann, and F.G. Hayden, *A release-competent influenza a virus mutant lacking the coding capacity for the neuraminidase active site*, J. Gen. Virol. 83 (2002), pp. 2683–2692.

[22] S. Gupta and R. Singh, *Analysis of the virus dynamics model reveals that early treatment of HCV infection may lead to the sustained virological response*, PLoS ONE 7 (2012), p. e41209.

[23] M.M. Hadjiandreou, R. Conejeros, and D.I. Wilson, *Long-term HIV dynamics subject to continuous therapy and structured treatment interruptions*, Chem. Eng. Sci. 64 (2009), pp. 1600–1607.

[24] B.G. Hale, A. Knebel, C.H. Botting, C.S. Galloway, B.L. Precious, D. Jackson, R.M. Elliott, and R.E. Randall, *CDK/ERK-mediated phosphorylation of the human influenza A virus NS1 protein at threonine-215*, Virology 383 (2009), pp. 6–11.

[25] A. Handel, I.M. Longini, and R. Antia, *Neuraminidase inhibitor resistance in influenza: Assessing the danger of its generation and spread*, PLoS Comput. Biol. 3 (2007), pp. 2456–2464.

[26] A.J. Hay, textitAmantadine and rimantadine — Mechanisms, in *Antiviral Drug Resistance*, D.D. Richman, ed., chap. 3, John Wiley & Sons Ltd, Chichester, England, 1996, pp. 43–58.

[27] F. Hayden, L. Jennings, R. Robson, G. Schiff, H. Jackson, B. Rana, G. McClelland, D. Ipe, N. Roberts, and P. Ward, *Oral oseltamivir in human experimental influenza b infection*, Antivir. Ther. 5 (2000), pp. 205–213.

[28] F.G. Hayden, *Amantadine and rimantadine — Clinical aspects*, in *Antiviral Drug Resistance*, D.D. Richman, ed., chap. 4, John Wiley & Sons Ltd, Chichester, England, 1996, pp. 59–77.

[29] C.-Q. He, N.-Z. Ding, X. Mou, Z.-X. Xie, H.-L. Si, R. Qiu, S. Ni, H. Zhao, Y. Lu, H.-Y. Yan, Y.-X. Gao, L.-L. Chen, X.-H. Shen, and R.-N. Cao, *Identification of three H1N1 influenza virus groups with natural recombinant genes circulating from 1918 to 2009*, Virology 427 (2012), pp. 60–66.

[30] G. He, J. Massarella, and P. Ward, *Clinical pharmacokinetics of the prodrug oseltamivir and its active metabolite Ro 64-0802*, Clin. Pharmacokin. 37 (1999), pp. 471–484.

[31] F.S. Heldt, T. Frensing, A. Pflugmacher, R. Gropler, B. Peschel, and U. Reichl, *Multiscale modeling of influenza A virus infection supports the development of direct-acting antivirals*, PLoS Comput. Biol. 9 (2013), p. e1003372.

[32] W. Henle, G. Henle, and E.B. RosenBerg, *The demonstration of one-step growth curves of influenza viruses through the blocking effect of irradiated virus on further infection*, J. Exp. Med. 86 (1947), pp. 423–437.

[33] W. Henle and E.B. RosenBerg, *One-step growth curves of various strains of influenza a and b viruses and their inhibition by inactivated virus of the homologous type*, J. Exp. Med. 89 (1949), pp. 279–285.

[34] B.P. Holder and C.A. Beauchemin, *Exploring the effect of biological delays in kinetic models of influenza within a host or cell culture*, BMC Public Health 11 (2011), pp. S10–S24 .

[35] N.H.G. Holford and L.B. Sheiner, *Understanding the dose-effect relationship: Clinical application of pharmacokinetic-pharmacodynamic models*, Clin. Pharmacokinet. 6 (1981), pp. 429–453.

[36] M.T. Hughes, M. Matrosovich, M.E. Rodgers, M. McGregor, and Y. Kawaoka, *Influenza A viruses lacking sialidase activity can undergo multiple cycles of replication in cell culture, eggs, or mice*, J. Virol. 74 (2000), pp. 5206–5212.

[37] H. Ikematsu, N. Kawai, N. Iwaki, and S. Kashiwagi, *In vitro neuraminidase inhibitory activity of four neuraminidase inhibitors against influenza virus isolates in the 2011-2012 season in Japan*, J. Infect. Chemother. 20 (2014), pp. 77–80.

[38] N.A. Ilyushina, N.V. Bovin, R.G. Webster, and E.A. Govorkova, *Combination chemotherapy, a potential strategy for reducing the emergence of drug-resistant influenza A variants*, Antiviral Res. 70 (2006), pp. 121–131.
[39] T. Jefferson, V. Demicheli, D. Rivetti, M. Jones, C.D. Pietrantonj, and A. Rivetti, *Antivirals for influenza in healthy adults: Systematic review*, Lancet 367 (2006), pp. 303–313.
[40] T. Jefferson, M. Jones, P. Doshi, C.D. Mar, L. Dooley, and R. Foxlee, *Neuraminidase inhibitors for preventing and treating influenza in healthy adults: a cochrane review*, Health Technol. Assess. 14 (2010), pp. 355–458.
[41] J. Kongkamnerd, L. Cappelletti, A. Prandi, P. Seneci, T. Rungrotmongkol, N. Jongaroonngamsang, P. Rojsitthisak, V. Frecer, A. Milani, G. Cattoli, C. Terregino, I. Capua, L. Beneduce, A. Gallotta, P. Pengo, G. Fassina, S. Miertus, and W. De-Eknamkul, *Synthesis and in vitro study of novel neuraminidase inhibitors against avian influenza virus*, Bioorg. Med. Chem. 20 (2012), pp. 2152–2157.
[42] H.C. Lim, M.E. Curlin, and J.E. Mittler, *HIV therapy simulator: A graphical user interface for comparing the effectiveness of novel therapy regimens*, Bioinformatics 27 (2011), pp. 3065–3066.
[43] C. Liu, M. Eichelberger, R. Compans, and G. Air, *Influenza type A virus neuraminidase does not play a role in viral entry, replication, assembly, or budding*, J. Virol. 69 (1995), pp. 1099–1106.
[44] B. Manicassamy, S. Manicassamy, A. Belicha-Villanueva, G. Pisanelli, B. Pulendran, and A. Garcia-Sastre, *Analysis of dynamics of influenza virus infection in mice using a GFP reporter virus*, Proc. Natl. Acad. Sci. USA 107 (2010), pp. 11531–11536.
[45] M.N. Matrosovich, T.Y. Matrosovich, T. Gray, N.A. Roberts, and H.D. Klenk, *Neuraminidase is important for the initiation of influenza virus infection in human airway epithelium*, J. Virol. 78 (2004), pp. 12665–12667.
[46] J.T. Nguyen, J.D. Hoopes, M.H. Le, D.F. Smee, A.K. Patick, D.J. Faix, P.J. Blair, M.D. Jongde, M.N. Prichard, and G.T. Went, *Triple combination of amantadine, ribavirin, and oseltamivir is highly active and synergistic against drug resistant influenza virus strains in vitro*, PLoS ONE 5 (2010), p. e9332.
[47] J.T. Nguyen, D.F. Smee, D.L. Barnard, J.G. Julander, M. Gross, M.D. Jongde, and G.T. Went, *Efficacy of combined therapy with amantadine, oseltamivir, and ribavirin against susceptible and amantadine-resistant influenza A viruses*, PLoS ONE 7 (2012), p. e31006.
[48] R. Padhi and J.R. Bhardhwaj, *An adaptive drug delivery design using neural networks for effective treatment of infectious diseases: A simulation study*, Comput. Meth. Programs Biomed. 94 (2009), pp. 207–222.
[49] L.T. Pinilla, B.P. Holder, Y. Abed, G. Boivin, and C.A.A. Beauchemin, *The H275Y neuraminidase mutation of the pandemic A/H1N1 influenza virus lengthens the eclipse phase and reduces viral output of infected cells, potentially compromising fitness in ferrets*, J. Virol. 86 (2012), pp. 10651–10660.
[50] C. Qiao, L. Liu, H. Yang, Y. Chen, H. Xu, and H. Chen, *Novel triple reassortant H1N2 influenza viruses bearing six internal genes of the pandemic 2009/H1N1 influenza virus were detected in pigs in China*, J. Clin. Virol. 61 (2014), pp. 529–534.
[51] M.N. Rahim, M. Selman, P.J. Sauder, N.E. Forbes, W. Stecho, W. Xu, M. Lebar, E.G. Brown, and K.M. Coombs, *Generation and characterization of a new panel of broadly reactive anti-ns1 mabs for detection of influenza A virus*, J. Gen. Virol. 94 (2013), pp. 593–605.
[52] G.F. Rimmelzwaan, M. Baars, E.C.J. Claas, and A.D.M.E. Osterhaus, *Comparison of RNA hybridization, hemagglutination assay, titration of infectious virus and immunofluorescence as methods for monitoring influenza virus replication in vitro*, J. Virol. Meth. 74 (1998), pp. 57–66.
[53] H.J. Schunemann, S.R. Hill, M. Kakad, R. Bellamy, T.M. Uyeki, F.G. Hayden, Y. Yazdanpanah, J. Beigel, T. Chotpitayasunondh, C.D. Mar, J. Farrar, T.T. Hien, B. özbay, N. Sugaya, K. Fukuda, N. Shindo, L. Stockman, G.E. Vist, A. Croisier, A. Nagjdaliyev, C. Roth, G. Thomson, H. Zucker, and A.D. Oxman, *WHO rapid advice guidelines for pharmacological management of sporadic human infection with avian influenza A (H5N1) virus*, Lancet Infect. Dis. 7 (2007), pp. 21–31.
[54] M. Sheikhan and S.A. Ghoreishi, *Antiviral therapy using a fuzzy controller optimized by modified evolutionary algorithms: a comparative study*, Neural Comput. Appl. 23 (2013), pp. 1801–1813.
[55] R.W. Sidwell and D.F. Smee, *In vitro and assay systems for study of influenza virus inhibitors*, Antiviral Res. 48 (2000), pp. 1–16.
[56] G.J. Smith, D. Vijaykrishna, J. Bahl, S.J. Lycett, M.W.O.G. Pybus, S.K. Ma, C.L. Cheung, J. Raghwani, S. Bhatt, J.M. Peiris, Y. Guan, and A. Rambaut, *Origins and evolutionary genomics of the 2009 swine-origin H1N1 influenza A epidemic*, Nature 459 (2009), pp. 1122–U107.
[57] C.-Y. Su, S.-Y. Wang, J.-J. Shie, K.-S. Jeng, N.J. Temperton, J.-M. Fang, C.-H. Wong, and Y.-S.E. Cheng, *In vitro evaluation of neuraminidase inhibitors using the neuraminidase-dependent release assay of hemagglutinin-pseudotyped viruses*, Antiviral Res. 79 (2008), pp. 199–205.
[58] A. Sugiura and E.D. Kilbourne, *Plaque formation by influenza viruses in a clone of a variant human heteroploid cell line*, Virology 26 (1965), pp. 478–488.
[59] Z. Tan, S. Akerstrom, B.Y. Wee, S.K. Lal, A. Mirazimi, and Y.-J. Tan, *A new panel of NS1 antibodies for easy detection and titration of influenza A virus*, J. Med. Virol. 82 (2010), pp. 467–475.
[60] J. Weiss, *The Hill equation revisited: uses and misuses*, FASEB J. 11 (1997), pp. 835–841.
[61] K.B. Westgeest, C.A. Russell, X. Lin, M.I.J. Spronken, T.M. Bestebroer, J. Bahl, R. Beekvan, E. Skepner, R.A. Halpin, J.C. Jongde, G.F. Rimmelzwaan, A.D.M.E. Osterhaus, D.J. Smith, D.E. Wentworth, R.A.M. Fouchier, and M. Graafde, *Genomewide analysis of reassortment and evolution of human influenza A(H3N2) viruses circulating between 1968 and 2011*, J. Virol. 88 (2014), pp. 2844–2857.
[62] N.T. Wetherall, T. Trivedi, J. Zeller, C. Hodges-Savola, J.L. McKimm-Breschkin, M. Zambon, and F.G. Hayden, *Evaluation of neuraminidase enzyme assays using different substrates to measure susceptibility of influenza virus*

clinical isolates to neuraminidase inhibitors: Report of the neuraminidase inhibitor susceptibility network, J. Clin. Microbiol. 41 (2003), pp. 742–750.

[63] Y. Wu, M. Zhang, J. Wu, X. Zhao, and L. Xia, *Evolutionary game theoretic strategy for optimal drug delivery to influence selection pressure in treatment of HIV-1*, J. Math. Biol. 64 (2012), pp. 495–512.

Appendix 1. Virus in the single cycle assay

In the single cycle assay, all cells are in the first compartment of the eclipse phase and there are no target cells. Thus, the equation for this phase reduces to

$$\frac{\mathrm{d}E_1}{\mathrm{d}t} = -\frac{n_E}{\tau_E}E_1, \tag{A1}$$

which is a simple exponential and has a solution of

$$E_1 = N\exp\left(-\frac{n_E t}{\tau_E}\right), \tag{A2}$$

where N is the number of cells in the well. We can then find the number of cells in any of the eclipse phase compartments by solving the series of differential equations. We find the general solution

$$E_n = \frac{1}{(n-1)!}\left(\frac{n_E}{\tau_E}\right)^{n-1} N t^{n-1}\exp\left(-\frac{n_E t}{\tau_E}\right). \tag{A3}$$

We can then substitute this expression into the differential equation for the first compartment of the infectious phase,

$$\frac{\mathrm{d}I_1}{\mathrm{d}t} = \frac{1}{(n_E-1)!}\left(\frac{n_E}{\tau_E}\right)^{n_E} N t^{n_E-1}\exp\left(-\frac{n_E t}{\tau_E}\right) - \frac{n_I}{\tau_I}I_1. \tag{A4}$$

While somewhat more complicated than the differential for any of the eclipse compartments, it basically has the same form. Since the number of eclipse cells in the nth compartment is a series of exponentials and the transition from one infectious compartment to another is exponential, the number of cells in any infectious compartment will also be a series of exponentials. It is important to note that the number of infected cells in any of the eclipse or infectious compartments is independent of the amount of virus and independent of the infection rate.

In the early times of the single cycle assay, before the viral peak, we can assume that viral clearance is negligible, so the differential equation for virus becomes

$$\frac{\mathrm{d}V}{\mathrm{d}t} = (1-n)p\sum_{j=1}^{n_I} I_j. \tag{A5}$$

Since the number of cells in any infectious compartment depends on time only, we can simply integrate this equation to get an expression for the virus as a function of time,

$$V = (1-n)p\int_{s=0}^{s=t}\sum_{j=1}^{n_I} I_j(s). \tag{A6}$$

The amount of virus is independent of the infection rate β, which explains why adamantanes do not show any effect in the single cycle assay. Virus is also linearly proportional to the NAI drug efficacy, so we can directly measure any NAI drug effect by measuring virus at any time before the peak.

Appendix 2. Cells in the incubation assay

In the incubation assay, the initial amount of virus is large and we assume that it remains approximately constant over the course of the experiment. Under this assumption, the equation for target cells becomes,

$$\frac{\mathrm{d}T}{\mathrm{d}t} = -\beta T V_0, \tag{A7}$$

which can be integrated to get an expression for the target cells,

$$T = T_0\exp(-\beta V_0 t). \tag{A8}$$

We then substitute this expression into the equation for the first compartment of the eclipse phase,

$$\frac{dE_1}{dt} = (1-m)\beta T_0 V_0 \exp(-\beta V_0 t) - \frac{n_E}{\tau_E} E_1, \tag{A9}$$

which has the solution

$$E_1 = \frac{(1-m)\beta V_0 T_0}{(n_E/\tau_E - \beta V_0)} \left(\exp(-\beta V_0 t) - \exp\left(-\frac{n_E t}{\tau_E} \right) \right). \tag{A10}$$

We can again find expressions for the number of cells in any eclipse compartment by recursively substituting into the differential equations. The general solution for the eclipse compartments is

$$E_n = \frac{(1-m)\beta V_0 T_0}{(n_E/\tau_E - \beta V_0)^n (n-1)!} \left[\Gamma\left(n, \left(\frac{n_E}{\tau_E} - \beta V_0 \right) t \right) - 1 \right] \exp(-\beta V_0 t), \tag{A11}$$

where Γ is the incomplete gamma function. We see that the number of cells in any eclipse compartment is linearly proportional to the adamantane drug effect. Note that the total number of eclipse cells will also be linearly proportional to the adamantane drug effect since we are simply summing over all eclipse compartments. We can find the number of infectious cells by continued integration of the differential equations, resulting in another series of exponentials, but the drug effect term will remain a multiplicative factor and will not be incorporated into any of the exponential functions.